Southern freshwater impacts and global ocean circulation

Bernd J. Haupt
Dan Seidov

E-mail: bjhaupt@psu.edu
dseidov@psu.edu
WWW: http://www.essc.psu.edu/~bjhaupt
http://www.essc.psu.edu/~dseidov

Earth & Mineral Science
Environment Institute

Introduction

The sensitivity of ocean circulation to changes in North Atlantic (NA) surface fluxes has become a major factor in explaining climate variability. The role of freshwater impacts in the Southern Ocean (SO) on the global ocean thermohaline circulation (THC) has received much less attention than such impacts in the northern North Atlantic (NA). Such a research bias limits the development of a complete understanding of decadal to millennial time–scale climate change. Our numerical experiments show that some additional freshwater at the sea surface in the SO can dramatically change the southern deepwater source and substantially alter the THC pattern. Additional analyses indicate that the Southern Hemisphere led the Northern Hemisphere changes in some of the glacial cycles of Pleistocene, implying a seesaw–type oscillation of the global ocean conveyor. The potential for melting of sea ice and ice sheets in the Antarctica associated with global warming can cause a further slowdown of the southern deepwater source. We present the results of systematic model simulation targeting the ocean circulation response to changes in surface salinity in the high latitudes of both Northern and Southern Hemispheres. We demonstrate that meltwater impacts in one hemisphere may lead to a strengthening of the thermohaline conveyor driven by the source in the opposite hemisphere. This, in turn, leads to significant changes in poleward heat transport. Further we show that THC restructuring can lead to deep–sea warming translating to thermal expansion of abyssal water, and thus causing a substantial sea level change even without a major ice sheet melting.

Figure 1: Stommel-Arons scheme of deep ocean currents.

Table 1: Amplitudes of sea surface salinity anomalies (in psu).

Exp.	NA	SO	WED	ANT	ACC
CRPDC (#1)	–	–	–	–	–
#2	-2.0	–	–	–	–
#3	–	-1.0	–	–	–
#4	-3.0	-1.0	–	–	–
#5	–	–	-3.0	–	–
#6	–	–	–	-1.0	–
#7	–	–	–	–	-1.0

CRPDC – Control Case (annual mean present –day sea surface climatology); NA – North Atlantic; SO – Southern Ocean; WED – the Weddell Sea; ANT – Antarctica coastline; ACC– ACC bound signal.
Salinity anomalies are added to the present –day annual mean sea surface salinity in the bands between 60°N and 80°N in NA, and/or 50°S and the coast of the Antarctica (SO). The modified salinity was merged using a cosine filter to the unchanged field within two latitudinal grid points (8°). In the SO the anomalies are circumglobal. The WED low salinity is confined to the Weddell Sea only. The ANT signal is in the band of 4° thickness around Antarctica; ACC is the signal in the band between around 50°S, approximate position of the ACC axes.

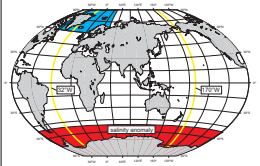

Figure 2: Idealized NA and SO meltwater events.

Table 2: Meridional overturning in the Atlantic Ocean (north of 30°S) in Sv ($1\ Sv = 10^6\ m^3/s$).

Exp.	NADW production	Convection depth in NA (km)	NADW outflow at 30°S	AABW inflow at 30°S
#1 (CRPDC)	16	3–4	10	6
#2 (NA-2 psu)	10	2	4	4
#3 (SO-1 psu)	25	bottom (> 4 km)	20	0
#4 (NA-3 +SO-1)	20	bottom (> 4 km)	14	4
#5 (WED-3 psu)	15	bottom (> 4 km)	10	4
#6 (ANT-1 psu)	20	bottom (> 4 km)	12	4
#7 (ACC-1 psu)	20	bottom (> 4 km)	12	4

Ocean bi-polar seesaw: Southern versus northern meltwater events

Model simulations demonstrate that meltwater impacts in one hemisphere may lead to strengthening of the thermohaline conveyor driven by the source in the opposite hemisphere. This leads to significant changes in poleward heat transport and to either deep-sea warming or cooling.

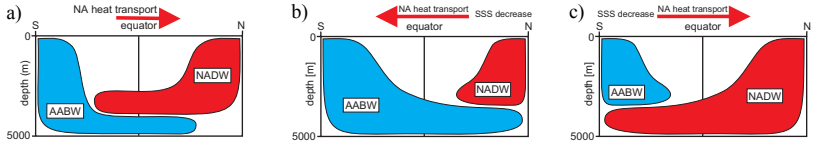

Figure 3: Schemes of water mass layering and overturning structure: (a) present–day; (b) present–day northern meltwater event; (c) present–day southern meltwater event. Direction of cross–equatorial oceanic heat transport is shown by arrows above each scheme.

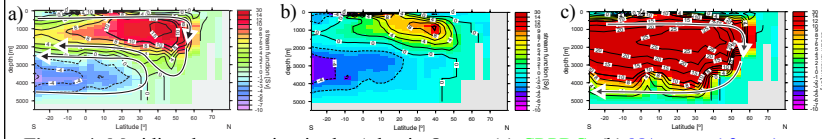

Figure 4: Meridional overturning in the Atlantic Ocean; (a) CRPDC; (b) NA event (-2 psu); (c) SO event (-1 psu) (see Table 1). Streamfunction is shown in Sv ($1\ Sv = 10^6\ m^3/s$).

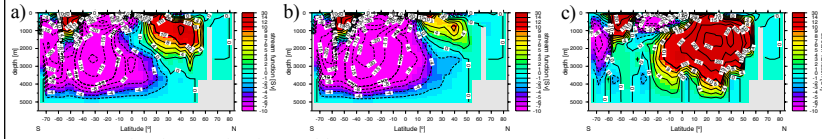

Figure 5: As in Figure 4 for the World Ocean.

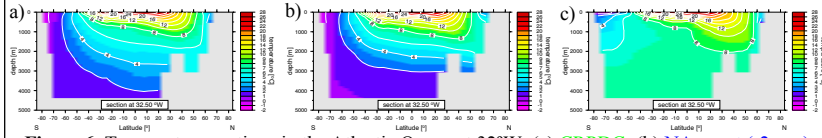

Figure 6: Temperature sections in the Atlantic Ocean at 32ºW: (a) CRPDC; (b) NA event (-2 psu); (c) SO event (-1 psu).

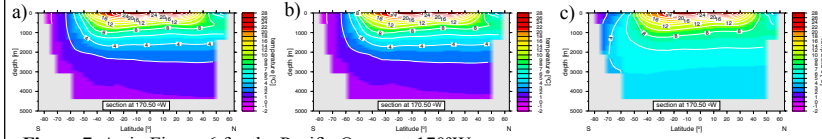

Figure 7: As in Figure 6 for the Pacific Ocean at 170ºW.

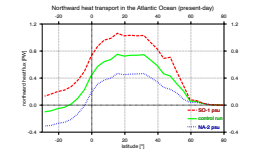

Figure 8: Northward heat transport (in PW; 1 PW = 10^{15} W) in the Atlantic Ocean in CRPDC (solid line), NA (-2 psu; dotted line), and SO (-1 psu; dash line) runs.

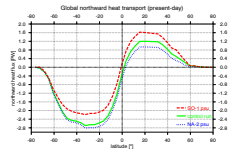

Figure 9: As in Figure 8 for the World Ocean.

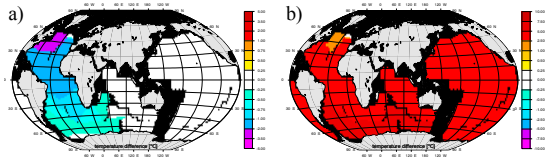

Figure 10: Temperature differences at 3000 m depth between (a) NA (-2 psu) and CRPDC experiments and (b) SO (-1 psu) and CRPDC experiments (see Table 1).

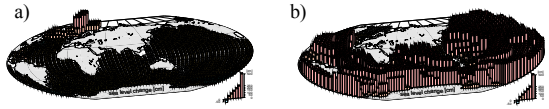

Figure 11: Sea level change in present–day NA (-2 psu) and SO (-1 psu) meltwater scenario (Exp. 2 and 3 in Table 1). Heights of the bars show the level change relative to the sea level in CRPDC run (Exp. 1 in Table 1).

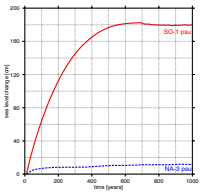

Figure 12: Evolution of the sea level change relative to the CRPDC sea level in time: solid line in SO (-1 psu) event, and dash line in NA (-2 psu) event.

References:

Seidov, D., B.J. Haupt, E.J. Barron, and M. Maslin, Ocean bi-polar seesaw and climate: Southern versus northern meltwater impacts, in The oceans and rapid climate change: Past, present, and future, edited by D. Seidov, B.J. Haupt, and M. Maslin, pp. 147-167, AGU, Washington, D.C., 2001.

Haupt, B.J., D. Seidov, and E.J. Barron, Glacial-to-interglacial changes of the ocean circulation and eolian sediment transport, in The oceans and rapid climate change: Past, present, and future, edited by D. Seidov, B.J. Haupt, and M. Maslin, pp. 169-197, AGU, Washington, D.C., 2001.

Seidov, D., E.J. Barron, and B.J. Haupt, Meltwater and the global ocean conveyor: Northern versus southern connections, Global and Planetary Change, 30 (3-4), 253-266, 2001.